Макрогетероциклы
http://mhc-isuct.ru

DOI: 10.6060/mhc245854s

Halogen-Free α,α-Bis(BODIPY) Bichromofore Photosensitizer: Synthesis, Spectral Properties and Water-Soluble Forms with Pluronic® F127 Micelles

Artem S. Sherudillo,[a] Lubov A. Antina,[a@] Valeria A. Kalinkina,[a,b] Alexander A. Kalyagin,[a] Alexander A. Ksenofontov,[a] Vasily M. Babaev,[c] Mikhail B. Berezin,[a] and Elena V. Antina[a]

[a]*G.A. Krestov Institute of Solution Chemistry of the Russian Academy of Sciences, 153045 Ivanovo, Russia*
[b]*Ivanovo State University of Chemistry and Technology, 153000 Ivanovo, Russia*
[c]*Arbuzov Institute of Organic and Physical Chemistry, FRC Kazan Scientific Center, Russian Academy of Sciences, 420088 Kazan, Russia*
[@]*Corresponding author E-mail: lyubov.antina@mail.ru*

In memory of O. I. Koifman – a unique leader of one of the leading scientific chemical schools, a Scientist, a Teacher, a man who with his works, amazing energy of the spirit and the power of his personality served and continues to serve as an example for each of us

BODIPY dyes are versatile molecules for designing new photosensitizers (PSs) or fluorescent theranostics for photodynamic therapy (PDT) and antimicrobial photodynamic therapy (APDT). BODIPY-based PSs are structural analogues of macrocyclic tetrapyrroles, which are currently the best known PSs and possess essential characteristics required for both PDT and APDT, including biocompatibility and excellent accumulation in cancer cells, as well as pronounced activity against various types of pathogenic microorganisms. BODIPY dimerization is a new method to create BODIPY PSs without heavy halogen atoms, which seem to be more attractive as PSs. The main features of the BODIPY dyads are determined by the positions of monomeric fragments attachment and the nature of the spacers connecting these domains. The results of the synthesis of the bichromophore α,α-bis(BDP) and its water-soluble form based on Pluronic® F127 micelles, the features of their structure, photophysical characteristics and solvatochromic effect are presented in this work. The α,α-bis(BDP) dye is characterized by high light absorption and strong excitonic splitting of the absorption low-energy band into the two high-intensity bands. Bichromophore α,α-bis(BDP) showed dual functionality due to relatively high fluorescence and singlet oxygen generation in aromatic and intermediate polarity solvents.

Keywords BODIPY bichromophore, fluorescence, intersystem crossing process, singlet oxygen generation, Pluronic® F127 micelles.

Негалогенированный бихромофорный фотосенсибилизатор α,α-bis(BODIPY): синтез, спектральные свойства и водорастворимые формы с мицеллами Pluronic® F127

А. С. Шерудилло,[a] Л. А. Антина,[a@] В. А. Калинкина,[a,b] А. А. Калягин,[a] А. А. Ксенофонтов,[a] В. М. Бабаев,[c] М. Б. Березин,[a] Е. В. Антина[a]

[a]*Институт химии растворов им. Г.А. Крестова Российской академии наук, 153045 Иваново, Россия*
[b]*Ивановский государственный химико-технологический университет, 153000 Иваново, Россия*
[c]*Институт органической и физической химии им. А.Е. Арбузова, ФИЦ Казанский научный центр РАН, 420088 Казань, Россия*
[@]*E-mail: lyubov.antina@mail.ru*

Памяти Оскара Иосифовича Койфмана – уникального Руководителя одной из ведущих научных химических школ, Ученого, Учителя, Человека, который своими трудами, потрясающей энергией Духа и мощью личности служил и продолжает служить примером для каждого из нас

BODIPY красители представляют собой универсальные молекулы для создания новых фотосенсибилизаторов (ФС) или флуоресцентных тераностиков для фотодинамической терапии (ФДТ) и антимикробной фотодинамической терапии (АФДТ). ФС на основе BODIPY являются структурными аналогами макроциклических тетрапирролов, которые на настоящее время являются наиболее известными ФС и обладают важными характеристиками, необходимыми как для ФДТ, так и для АФДТ, включая биосовместимость и селективное накопление в раковых клетках, а также выраженную активность в отношении различных видов патогенных микроорганизмов. Димеризация BODIPY красителей является новым методом получения ФС на основе BODIPY и не требует дополнительного включения тяжелых атомов галогенов. Ключевые особенности свойств BODIPY бихромофоров определяются позициями присоединения мономерных фрагментов и природой связывающего спейсера, соединяющих эти домены. В настоящей работе представлены результаты синтеза α,α-bis(BDP) бихромофора и его водорастворимой формы на основе мицелл плюроника F127, исследования особенностей их структуры, фотофизических характеристик, сольватохромного эффекта. Краситель α,α-бис(BDP) характеризуется высоким светопоглощением и сильным экситонным расщеплением низкоэнергетической полосы спектра поглощения на две высокоинтенсивные полосы. Бихромофор α,α-бис(BDP) продемонстрировал двойную функциональность благодаря относительно высокой флуоресценции и генерации синглетного кислорода в ароматических растворителях и среднеполярных растворителях.

Ключевые слова BODIPY бихромофор, флуоресценция, интеркомбинационная конверсия, генерация синглетного кислорода, мицеллы плюроника F127.

Introduction

Classical alkyl-substituted BODIPY luminophors typically exhibit intense fluorescence but lack significant phosphorescence.[1] The simplest and most well-known strategy for partial energy redistribution from the excited singlet state to the triplet state is the “heavy atom effect” due to the introduction of bromine or iodine atoms into the BODIPY molecules.[2–4] Another way is BODIPY dimerization to create heavy-atom-free BODIPY PSs, which seem to be more appealing as PSs due to the low dark toxicity.[5-7] Several papers have already been published devoted to the preparation of BODIPY bichromophore-based photosensitizers.[3–6,8-10] Turns out, the main features of the BODIPY dyads are determined by the positions of monomeric fragments attachment and the nature of the spacers connecting these domains. Both the probability and efficiency of exciton interactions, fluorescence, intersystem crossing process and consequently the possibility of singlet oxygen generation depend on it. The general feature of most alkyl-substituted BODIPY bichromophores is the high sensitivity of their fluorescence characteristics to solvent polarity, which is also of interest for biomedical applications.[10–15] However, not all BODIPY bichromophores are able to generate singlet oxygen, but mainly BODIPY domains are orthogonally arranged, leading to intersystem crossing (ISC) process. But the disadvantage of BODIPY dyads is a more difficult synthesis procedure with low yields. Moreover, high hydrophobicity of BODIPY-based PSs, including bichromophoric ones, requires selection of an optimal biocompatible delivery system for further use in biomedicine. At the same time, the rather large sizes of dyad molecules complicate the task of choosing their delivery systems. For instance, most MOF systems, including ZIF-8, recommended as a delivery system for bioactive molecules and drug compounds, are not suitable due to insufficiently large channels and cavity sizes.[16,17] Previously, we have shown that BODIPY bichromophores are sufficiently solubilized by micelles of the biocompatible amphiphilic block copolymer Pluronic® F127. It is known for its low toxicity and typically allows for high solubilization efficiency while maintaining the important spectral properties of loaded photoactive compounds in an aqueous (physiological) environment.

Therefore, this study is focused on the synthesis of decamethyl-substituted α,α-bis(BODIPY) bichromophore (Figure 1) and preparation of its water-soluble forms α,α-bis(BDP)@Pl, analyzing their photophysical, aggregation characteristics and solvent effect.

In molecules of alkyl-substituted BODIPY-BODIPY dyads formed by bonding monomeric domains through α,α-positions of proximal pyrroles by a methylene bridge[15,18] or directly by sigma bonding,[11,14,19] conditions for effective interaction of dipoles of closely arranged units are created. It leads to a vivid manifestation of exciton splitting of the intense band in the electronic absorption spectrum. There is practical potential for such compounds for applications in optics and photovoltaics as well as in biomedicine.

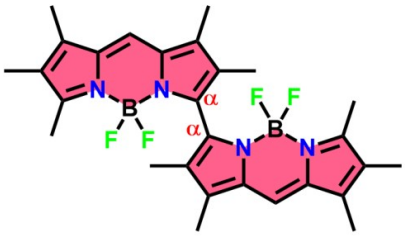

Figure 1. Object of study – α,α-bis(BDP).

Experimental

Materials and methods

All organic solvents used were of spectrophotometric grade (for analysis, Panreac, Barcelona) and were used without further purification. Pluronic® F127 (PEO100-PPO65-PEO100) was obtained from Sigma-Aldrich (USA). The ^{1}H spectra were obtained using a Bruker Avance-III 500 MHz spectrometer to determine the bis(BODIPY)s structure. The operating frequency for the cores was 500.17 MHz. Sample preparation was done in standard NMR ampoules (OD = 5 mm) with deuterated chloroform as a solvent and a small amount (0.03 v/v %) of TMS as an internal standard. The temperature was maintained at 25 °C using temperature control units (Bruker BVT-2000) and cooling units (Bruker BCU 05). All NMR spectra were recorded using the pulse programs included in the software package of the TopSpin 3.6.1 spectrometer. The ^{1}H NMR spectra were recorded in the spectral range of 12.4 ppm, with 32 scans, a relaxation delay (d1) of 3 seconds, and 32768 data points. The MALDI mass spectra were recorded on an Ultraflex III TOF/TOF mass spectrometer (Bruker Daltonic GmbH, Bremen, Germany). The data was obtained using the FlexControl program (Bruker Daltonik GmbH, Germany) and processed using the FlexAnalysis 3.0 program (Bruker Daltonik GmbH, Germany).

Photophysical properties

The electronic absorption spectra of compound solutions were recorded on a CM 2203 spectrometer (SOLAR) in the range of molar concentrations from 10^{-7} to 10^{-5} mol/L at 25 ± 0.1 °C. The fluorescence spectra of dye solutions were recorded on a CM 2203 spectrometer (SOLAR) and FluoTime 300 (PicoQuant, Germany). The fluorescence quantum yield, fluorescence lifetime, radiative (k_{rad}), and non-radiative (k_{nr}) process constants were determined using a methodology similar to our previous reports.[20] The fluorescence quantum yield (Φ_{fl}) of α,α-bis(BDP) solutions in organic solvents was determined using Rhodamine 6G in ethanol as a reference. The fluorescence quantum yield (Φ_{fl}) of α,α-bis(BDP)@Pl in PBS was determined on a FluoTime 300 spectrometer (PicoQuant, Germany) with a laser LDH-P-C-500 (PicoQuant) as an excitation source and an integration sphere. The time-resolved fluorescence measurements were carried out by means of FluoTime 300 spectrometer (PicoQuant) with a laser LDH-P-C-500 (PicoQuant) as an excitation source. The instrument response function (IRF) of the system was measured using the stray light signal of the dilute colloidal silica suspension (LUDOX®). The fluorescence decay of α,α-bis(BDP) were measured, and the fluorescence lifetimes were obtained by reconvolution of the decay curves using the EasyTau 2 software package (PicoQuant, Germany). The singlet oxygen generation was determined by direct measurement of the luminescence at 1275 nm with a spectrometer FluoTime 300 (PicoQuant), equipped NIR detector (laser LDH-P-C-500 (PicoQuant) as the excitation source). Measurements were taken in cuvettes with a path length of 1 cm. The signal was filtered by a cut-off wavelength of 1050 nm. The singlet oxygen quantum yield (Φ_Δ) was determined using Equation (1),[8] the excitation was at 500 nm and two reference were used: rose bengal (Φ_Δ = 0.53 in ACN, Φ_Δ = 0.68 in ethanol, Φ_Δ =0.76 in D_2O) and tetraphenylporphine (Φ_Δ = 0.62 in benzene, Φ_Δ = 0.62 in THF, Φ_Δ = 0.55 in chloroform and Φ_Δ = 0.64 in DMF [8,21]):

$$\Phi_{\Delta PS} = \Phi_{\Delta st} \cdot (\alpha_{st}/\alpha_{PS}) \cdot (Se_{PS}/Se_{st}), \quad (1)$$

where $\Phi_{\Delta st}$ is the Φ_Δ corresponding reference; factor $\alpha = 1\text{-}10^{-Abs}$, corrects the different amounts of photons absorbed by the sample (α_{PS}) and reference (α_{st}); *Se* is the $^1O_2$ signal of the α,α-bis(BDP) or α,α-bis(BDP)@Pl and the reference at 1275 nm. $^1O_2$ quantum yields were averaged from several concentrations.

DFT calculations

At the first stage, conformational screening was carried out for α,α-bis(BDP) by GFN2-xTB in the CREST package.[22] Next, the potential energy surface was scanned *vs.* the torsional angle of α,α-bis(BDP) using ωB97X-D/def2-SVP.[23,24] For α,α-bis(BDP) the most stable conformer was determined and its geometry was optimized in the ground, first excited singlet, and triplet states using ωB97X-D/def2-TZVP and UωB97X-D/def2-TZVP, respectively[24] (Tables S1 – S3, *Supplementary Information*). Energy minima of optimized geometry were confirmed by absence of the imaginary frequencies. At the same level of theory, TDDFT analysis was performed for α,α-bis(BDP). In TDDFT calculation, the first 50 singlet excited states were calculated. The influence of chloroform on the energy, structural and spectral characteristics was taken into account in the SMD model.[25] All DFT/TDDFT calculations were carried out in the Gaussian 16 software package. The ChemCraft 1.8 was used to analyze the results and molecular graphics.[26]

Synthesis

5,5-Bis(BF$_2$-pentamethyl-2,2'-dipyrromethene), (α,α-bis(BDP)) (*M*=522.20 g/mol) was synthesized according to the procedure described earlier.[27] 0.231 g (1.426 mmol) of anhydrous $FeCl_3$ was added to a solution of 0.1869 g (0.713 mmol) of BF_2-pentamethyl-dipyrromethene in 30 mL of dry dichloromethane cooled in an ice bath. The initially orange solution quickly turned dark red. After 2 min, the reaction was quenched by adding 40 mL of methanol and stirred for another 20 min. The organic phase was washed with water (2×50 mL), dried over anhydrous Na_2SO_4 and evaporated to dryness on a rotary evaporator. The solid residue was separated by column chromatography on silica gel. First, the chromatogram was eluted with a mixture of CH_2Cl_2/hexane = 1:1, and unreacted BF_2-pentamethyldipyrromethene was separated in the form of an orange fraction with yellow-green fluorescence (0.1727 g, 0.658 mmol of the adduct was returned, which was used for repeated syntheses. 0.055 mmol of the starting substance reacted). The column was then eluted with pure CH_2Cl_2, releasing a red-violet fraction with red fluorescence. The solvent was removed to obtain 11.7 mg (0.022 mmol, 40%) of the dimer. Mass spectrum, *m/z*: 503.2 $[M^-F]^+$, 522.2 $[M^+]$, 545.2 $[M^+Na]^+$. ^{1}H NMR ($CDCl_3$) δ ppm: 7.16 (s, 2H, *ms*-H); 2.37 (s, 6H, CH_3); 2.26 (s, 6H, CH_3); 2.18 (s, 6H, CH_3); 1.93 (s, 6H, CH_3); 1.81 (s, 6H, CH_3).

The α,α-bis(BDP) loaded Pluronic® F127 micelles α,α-bis(BDP)@Pl were prepared by thin-film method similar to the presented in [12]. Pluronic® F127 in THF was added to a solution of α,α-bis(BDP) of a given concentration in THF and the mixture was kept for 2 hours at a temperature of 37 °C with stirring. The solvent was then removed using a rotary evaporator, the resulting α,α-bis(BDP)@Pl films were stored in the dark (or collected as a powder for long-term storage) and dissolved in phosphate buffer (PBS, p*H* 7.4) or D_2O before spectral analysis. Suspensions of α,α-bis(BDP)@Pl in phosphate-buffered saline (PBS, p*H* 7.4) were centrifuged to remove unsolubilized dye but were not passed through filters to carry out a complete analysis of the formed polymer particles size.

Results and Discussion

Photophysical characteristics of α,α-bis(BDP) in organic solvents

It is known that for closely-spaced bichromophoric BODIPY derivatives excitonic coupling splits the lowest-energy absorption transition. The exciton splitting is highly variable degrees depending on the mode of binding, including the site of attachment. The α,α-bis(BDP) is

characterized by a strong manifestation of excitonic interactions and a strong splitting of the low-energy band of the absorption spectrum into two high-intensity major bands at 553 – 564 nm and 482 – 492 nm respectively, shifted in red and blue region relative to the S_0-S_1 band of the hexamethyl-substituted monomer (Figure 2a, Table 1, Figure S1, *Supplementary Information*). No concentration effect could be detected in the range of 5 – 50 μM (Figure 2b), indicating that there is no aggregation in this range and that the exciton splitting detected has an intramolecular origin. The values of extinction coefficients are high (lgε is 4.78 – 4.83 depending on the solvent, determined in the solvents with a fairly high solubility of the dye), which indicates its high light-absorbing ability (Table 1).

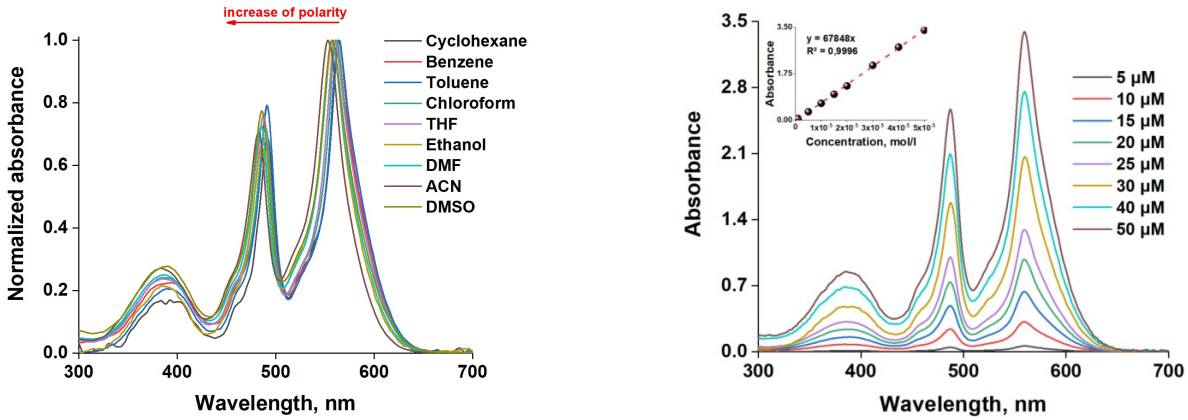

a *b*

Figure 2. Normalized absorption spectra of α,α-bis(BDP) in organic solvents (*a*) and absorption spectra in THF with different concentrations of α,α-bis(BDP) (*b*).

Table 1. Spectral characteristics of α,α-bis(BODIPY) in different solvents.

Solvent	λ_{abs}, nm; (lgε)	$\Delta\nu_{ES}$, cm^{-1}	$\Delta\nu_{SS}$, cm^{-1}	λ_{fl}, nm	τ_{fl},ns	$k_{rad} \cdot 10^{-8}$, s^{-1}	$k_{nrad} \cdot 10^{-8}$, s^{-1}	Φ_{fl}	Φ_{Δ}
Cyclohexane	564; 492; 389	2595	2298	648	3.44	1.61	1.30	0.55	-
Benzene	564; 491; 388	2636	2417	653	3.32	1.19	1.82	0.39	0.50
Toluene	564; 491; 389	2636	2370	651	3.32	1.20	1.81	0.40	-
Chloroform	561 (4.88); 489; 388	2625	2441	650	3.41	1.27	1.66	0.43	0.33
THF	560 (4.83); 488; 387	2635	2473	650	3.22	1.05	2.06	0.34	0.87
Ethanol	558; 486; 386	2655	2537	650	1.05	1.08	8.47	0.11	0.06
DMF	557 (4.78); 485; 386	2665	2639	653	0.82	0.93	11.25	0.076	0.02
ACN	553; 482; 384	2664	2675	649	0.39	0.94	24.50	0.037	0.13
DMSO	557; 486; 388	2623	2709	656	0.58	0.86	16.31	0.050	-

Note: absorption maxima (λ_{abs}, nm), molar absorption coefficients (lgε), exciton splitting ($\Delta\nu_{es}$, cm^{-1}), emission maxima (λ_{fl}, nm), Stokes shift ($\Delta\nu_{SS}$, cm^{-1}), fluorescence quantum yield (Φ_{fl}), fluorescence lifetime (τ_{fl}, ns), radiative constants (k_{rad}, s^{-1}), non-radiative constants (k_{nrad}, s^{-1}) singlet oxygen generation quantum yield (Φ_{Δ}).

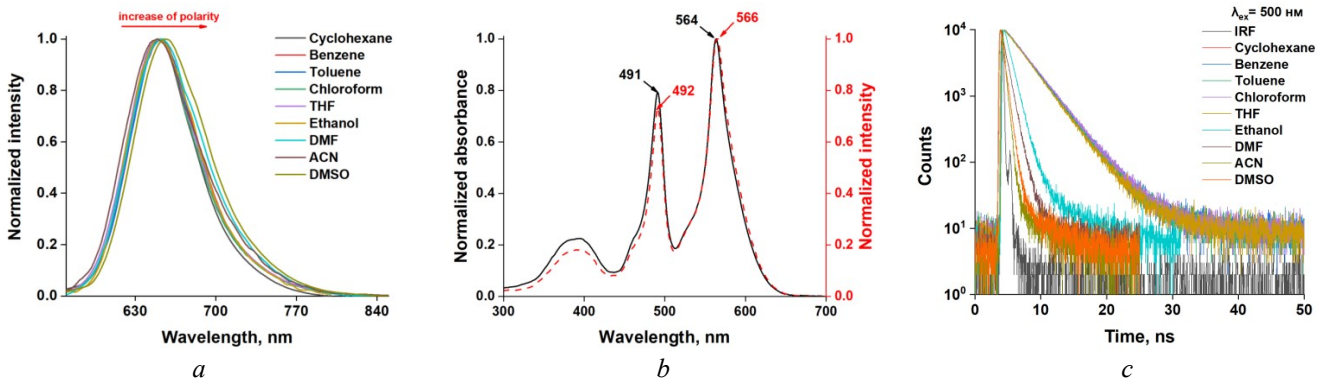

a *b* *c*

Figure 3. Fluorescence spectra of α,α-bis(BDP) in organic solvents (*a*); excitation spectrum (dot) registered at 653 nm and normalized absorption spectrum of α,α-bis(BDP) benzene (*b*), time resolved fluorescence decays of α,α-bis(BDP) in organic solvents (*c*).

It can be noted that a slight dependence of α,α-bis(BDP) on solvent polarity was observed. When moving from inert non-polar (cyclohexane) and aromatic (benzene, toluene) solvents to polar proton- (ethanol) and electron-donating (DMF, DMSO) solvents, the values of absorption maximum according to the low-energy spectral bands are blue-shifted to 7 nm (Table 1).

The fluorescence spectra of α,α-bis(BDP) have a broad emission bands and are strongly shifted with respect to the lowest-energy absorption (Figure 3a). The Stokes shift values are large and increase from 2298 cm^{-1} to 2623 cm^{-1} (Table 1). The excitation spectra, registered on the emission maxima of the α,α-bis(BDP), ideally match the absorption spectra (Figure 3b), which indicates a true emission of the bichromophore. The broad emission spectra and large values of the Stokes shift (Table 1) indicate large energy losses, possibly due to strong structural rearrangements in the excited state compared to the ground state (which will be shown below based on the results of DFT calculations).

To elucidate the nature of the bands in the absorption spectra and the spectral behavior of α,α-bis(BDP) in both ground and excited states, DFT and TDDFT calculations were carried out. By scanning the potential energy surface for α,α-bis(BDP) as the torsion angle function, two conformers were identified. These conformers undergo a transformation into each other when one BODIPY moiety is rotated relative to the other by 180 deg. (Figure S2, *Supplementary Information*). The most energetically favorable conformer of α,α-bis(BDP) is stabilized by intramolecular interactions between the fluorine atom of one BODIPY moiety and the hydrogen atom of the α-methyl group of another BODIPY moiety (~2.700 Å). The dihedral angle between the planes of the BODIPY moieties in the ground (S_0) state of α,α-bis(BDP) is 85 deg. The nearly orthogonal orientation of the BODIPY moieties enhances the excitonic interaction efficiency,[11,28] as evidenced by the pronounced splitting of the intense long-wavelength band in the absorption spectrum observed experimentally (Figure 2). In the first singlet (S_1) excited state of α,α-bis(BDP), a decrease in the dihedral angle to 82 deg. is observed. The geometry of α,α-bis(BDP) in the first triplet (T_1) excited state is close to the geometry of the S_0 state, with a dihedral angle of 84 deg (Figure S3, *Supplementary Information*). Furthermore, as depicted in Figure S3 the geometry of α,α-bis(BDP) in the S_0 state shows significant deviation from that in the S_1 state, potentially accounting for the experimentally recorded large the Stokes shift values (Table 1). The dipole moment (μ) of α,α-bis(BDP) in the S_0 and S_1 states is respectively 1.45 D and 1.51 D. The insignificant difference between them may suggest reasons for the experimentally observed weak sensitivity of the absorption band maximum of α,α-bis(BDP) to solvent polarity (Table 1). However, $\mu_{S0} < \mu_{S1}$, which experimentally should most likely manifest itself in the positive solvatochromism form.[29] But, in the case of α,α-bis(BDP), with increasing solvent polarity, the absorption band maximum shifts to the blue spectrum region. This may be due to the dominance of specific solvation, characteristic of BODIPY dimers, over the universal one.[15,18]

TDDFT analysis of α,α-bis(BDP) enabled the explanation of the electronic transitions nature in the experimental absorption spectra (Figure S4, Table S4, *Supplementary Information*). The most probable HOMO–LUMO and HOMO–LUMO+1 electronic transitions contribute significantly to the α,α-bis(BDP) spectral properties. These electronic transitions are associated with the delocalization of electron density throughout the entire α,α-bis(BDP) molecule.

The fluorescence quantum yield of α,α-bis(BDP), as for most BODIPY bichromophores, is highly sensitive to the solvent nature (Table 1). The fluorescence efficiency is relatively high in non-polar inert solvents ($\Phi_{fl} = 0.55$ in cyclohexane). The modest fluorescence efficiency is observed in aromatic solvents ($\Phi_{fl} = 0.39$ and 0.40 in benzene and toluene) and intermediate polarity solvents ($\Phi_{fl} = 0.43$ and 0.34 in chloroform and THF). The fluorescence efficiency is greatly decreases as the polarity of the solvent increases ($\Phi_{fl} = 0.11$ in ethanol, $\Phi_{fl} = 0.076$ in DMF, $\Phi_{fl} = 0.05$ in DMSO and 0.037 in ACN). In apolar (cyclohexane, benzene, toluene) and intermediate polarity solvents (chloroform and THF) a monoexponential decay curve with a fluorescence lifetime of around 3.2–3.4 ns was produced (Figure 3c, Tables 1 and S2). Two exponentials are required to fit the decay curves of α,α-bis(BDP) (Tables 1 and S1, Figure 3c) in other, more polar solvents excluding acetonitrile. Thus, the fluorescence lifetime of α,α-bis(BDP) has two components in ethanol, DMF and DMSO: a long component (τ_2 is 2.67–4.57 ns) which is related to the radiative deactivation from the excited state; a short component (τ_1 is 0.51–0.98 ns), giving the maximum contribution to the total lifetime, which could be related to a non-radiative process such as specific interactions of the dye with proton- and electron-donating solvent molecules and intersystem crossing to the triplet state (Table S2, *Supplementary Information*). In ACN the fluorescence lifetime was fitting on three components: τ_2 = 4.39 ns and two short-lived 0.15 ns and 0.39 ns (Table S2).

For α,α-bis(BDP), $^1O_2$ luminescence spectra were recorded and the quantum yield of singlet oxygen generation (Φ_Δ) was calculated in several solvents. The Φ_Δ values are also highly sensitive to the nature of the solvent: α,α-bis(BDP) generates efficiently in the intermediate polarity THF ($\Phi_\Delta = 0.87$) and chloroform ($\Phi_\Delta = 0.33$), aromatic non-polar benzene (Φ_Δ = 0.50) and greatly decreases till 0.02–0.10 in polar (acetonitrile, DMF, ethanol) (Table 1). Thus, we have experimentally shown that α,α-bis(BDP) is one of the few representatives of heavy-atom-free photosensitizers capable of efficient generation of singlet oxygen. Moreover, α,α-bis(BDP) in aromatic and intermediate polar solvents shows dual functionality related to a relatively high fluorescence and singlet oxygen generation. To elucidate this phenomenon nature, we calculated the energy gap between the lowest singlet excited state (S_1) and the lowest triplet state (T_1) (ΔE_{S1T1}). It is known that decreasing the ΔE_{S1T1} value enhances the intersystem crossing (ISC) efficiency.[12,30] The ΔE_{S1T1} value for α,α-bis(BDP) was 1.06 eV. This value is lower than, for example, the value of $\Delta E_{S1T1} = 1.38$ eV for a heavy-atom-free photosensitizer based on β',β'-CH_2-bis(BDP), in which, according to our data, spin–orbit charge-transfer-induced intersystem crossing (SOCT-ISC) occurs.[12] This indicates a higher efficiency of ISC for α,α-bis(BDP). The highest efficiency in singlet oxygen generation for α,α-bis(BDP) is observed in aromatic and weakly polar solvents. Analysis of the frontier molecular orbitals (FMO) of α,α-bis(BDP) in the T_1 state (Figure 4) suggests the potential formation of a state with intramolecular charge transfer (CT state).

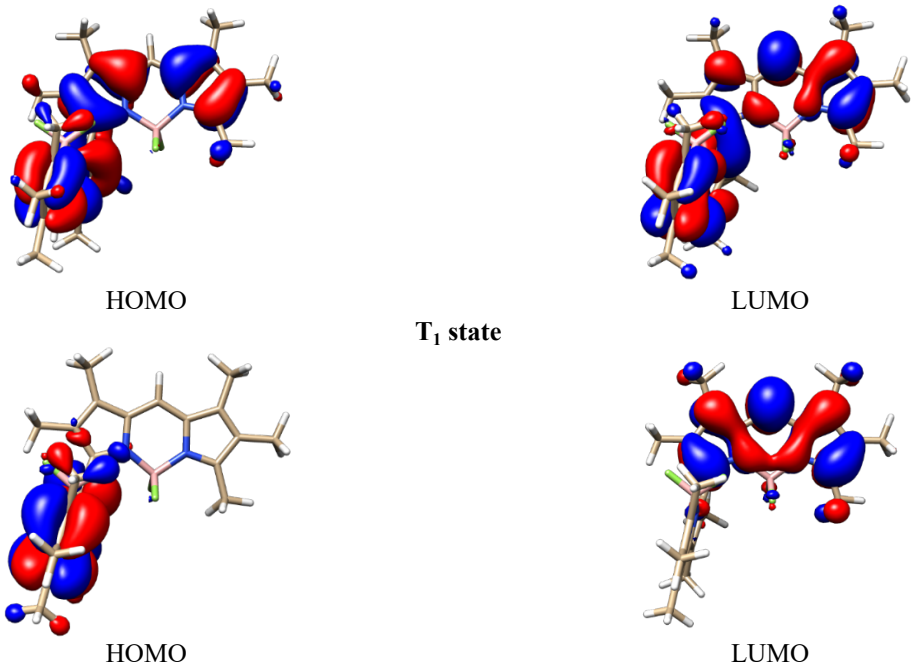

Figure 4. The FMOs type of α,α-bis(BDP) in S_0, S_1, and T_1 state.

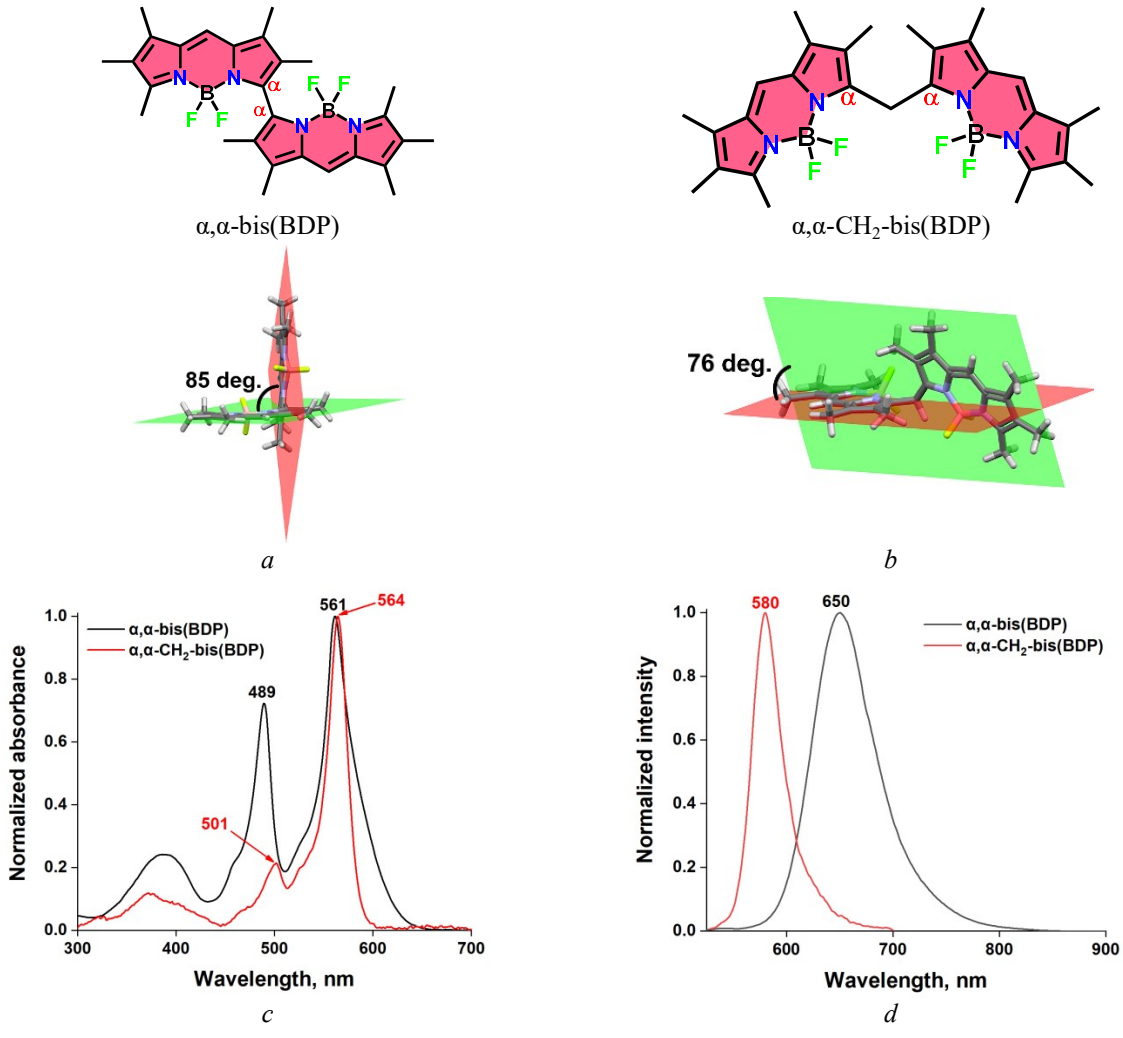

Figure 5. The optimized structures and dihedral angles between BODIPY unit planes of α,α-bis(BDP) (*a*) and α,α-CH_2-bis(BDP) (*b*)[12]; normalized absorption (*c*) and fluorescence (*d*) of α,α-bis(BDP) and α,α-CH_2-bis(BDP) in chloroform.

The combination of this factor with the high value of the dipole moment (μ_{T1} = 1.89 D) in the T_1 state should lead to the stabilization of the CT state in highly polar solvents, resulting in the ISC efficiency decrease and, consequently, a significant reduction of $^1O_2$ generation due to the competition between the two mechanisms (Table 1). By decreasing the solvent polarity, the CT state efficiency is reduced. This leads to ISC process efficiency increase, consequently enhancing the singlet oxygen quantum yield, which reaches its maximum value in THF (Table 1). However, in nonpolar solvents, the CT state efficiency is significantly reduced, resulting in maximum fluorescence and decrease $^1O_2$ generation. The results of quantum chemical calculations are consistent with the experimentally observed values of Φ_{fl} and Φ_Δ (Table 1), as well as with the discovered sensitivity of fluorescence characteristics and singlet oxygen generation to solvent polarity.

Comparison of the α,α-bis(BDP) and α,α-CH_2-bis(BDP) dyads structure and photophysical characteristics

Previously, we presented the results of a detailed analysis[12,15,18] (Table S3, *Supplementary Information*) of the molecular structure and photophysical properties features of the dyad with a methylene spacer (Figure 4). The α,α-bis(BDP) and α,α-CH_2-bis(BDP) bichromophores have identical pyrroles alkyl substitution and site of attachment BODIPY units, but in α,α-CH_2-bis(BDP) the chromophoric domains are linked via CH_2-spacer.

The dihedral angle between BODIPY fragments for α,α-CH_2-bis(BDP) in the ground (S_0) state is 75.95 deg (Figure 5a), which is 10 degrees less compared to α,α-bis(BODIPY) (Figure 5b). Unlike α,α-bis(BDP), BODIPY units in the α,α-CH_2-bis(BDP) molecule are located non-orthogonally and at a greater distance. Therefore, for α,α-CH_2-bis(BDP) excitonic interactions are less pronounced, the value of long-wavelength absorption band exciton splitting is 2176–2207 cm^{-1}, which is noticeably lower compared to 2595–2623 cm^{-1} for α,α-bis(BDP); the positions of the S_0-S_1 bands are close (Figure 5c), but the intensity ratio $A_{S0\text{-}S2}/A_{S0\text{-}S1}$ for α,α-CH_2-bis(BDP) is much lower compared to α,α-bis(BDP). The maximum of the α,α-bis(BDP) fluorescence band is located on average 70 nm more bathochromically, and the Stokes shift values are on average approximately four times higher compared to α,α-CH_2-bis(BDP) due to the large energy losses in excited state (Figure 5d). Both compounds are characterized by solvent polarity dependent fluorescence and its strong quenching to approximately the same Φ_f values in solutions of polar proton and electron donor solvents. The Φ_{fl} values for α,α-CH_2-bis(BDP) in low-polar and non-polar solvents are 0.58 (THF), 0.87 (benzene), 0.95 (chloroform) and 0.99 (cyclohexane), which is more than twice as high as compared to with α,α-bis(BODIPY). The value of ΔE_{S1T1} α,α-CH_2-bis(BDP) is 4.50 eV, which is four times higher than the value (ΔE_{S1T1} is 1.06 eV) four α,α-bis(BODIPY). Large values of ΔE_{S1T1} exclude the possibility of intersystem crossing (ISC), which explains the intense fluorescence of α,α-CH_2-bis(BDP) in non-polar and intermediate polarity solvents and the almost complete absence of singlet oxygen generation in all studied solvent.

Thus, the attachment style in BODIPY–BODIPY dyads has a strong influence on the exciton interactions efficiency and photophysical characteristics: the connection of domains through a methylene bridge allows achieving intense fluorescence, directly connection to achieve partial redistribution of energy into the triplet and satisfactory generation of singlet oxygen and fairly effective fluorescence.

Aggregation behavior of α,α-bis(BDP) in a THF-water mixture

Since α,α-bis(BDP) is insoluble in water, its introduction into biological objects involves the use of a mixture of an organic solvent with an aqueous buffer solution under conditions of a minimum content of the organic component. But the high hydrophobicity and aromaticity of the BODIPY molecule determines a high tendency to intense aggregation in aqueous-organic systems, leading to an unfavorable distortion of their practically significant photophysical characteristics. It is important to take into account that the intensity of aggregation processes and the type of aggregates formed depend on the features of the functionalization of BODIPY molecules[31].

To develop ideas about possible changes in spectral characteristics during aggregation in solutions, we analyzed the aggregation behavior of α,α-bis(BDP) in THF-water mixtures that are most convenient for carrying out this type of study. A series of THF-water solutions were prepared in which the dye concentration constant was remained ($C_{\alpha,\alpha\text{-bis(BDP)}}$ = 6.5 μM), the volumetric water content (f_w) increased from 0 to 95 v/v %. Figure 5 shows the recorded absorption and fluorescence spectra of α,α-bis(BDP) in the THF-water mixtures.

In the case of α,α-bis(BDP), the nature of spectral transformations in aqueous-organic media is very specific. Analysis of the obtained results showed that for the α,α-bis(BDP) molecule there is no intense formation of H-type aggregates, which should be accompanied by a hypochromic effect and a blue shift of the absorption band maximum compared to a solution of the dye in pure THF, which is typical, for example, for the mononuclear hexamethyl substituted BODIPY and other classical alkyl substituted monochromophores BODIPY.[32] In addition, it is impossible to unambiguously state the formation of *J*-type aggregates, which should have been accompanied by a red shift of the maximum of the absorption band of the dye or the formation of a new longer wavelength band, as well as the possible appearance of an additional emission band, which was observed for some BODIPYs functionalized with bulky substituents,[33] as well as for β',β'-CH_2-bis(BDP).[12,31]

An increase in water content from 0 to 50 v/v % does not lead to noticeable changes in the absorption spectra of α,α-bis(BDP) (Figure 6a). With a further increase in water content, a sharp decrease in the absorption intensity of the dye is observed due to a decrease in its solubility and a strong broadening of the S_0-S_1 absorption band. With a further increase in water content (f_w > 50 v/v %), there is no clear trend in the shift of the absorption maximum of the intense band (Figure 6b). At f_w = 95 v/v %, the maximum S_0-S_1 absorption band of the α,α-bis(BDP) is located around

555 nm, *i.e.* slightly shifted to the blue region of the spectrum (5 nm) compared to the dye in pure THF, which may be due to a change in the nature of the solvation environment (Figure 6a). In addition, in the spectra of solutions with f_w > 50 v/v %, the S_0-S_2 band at 488 nm disappears and a new band appears at 501 nm, which may be due to rearrangements in the structure of α,α-bis(BDP) molecules. Thus, with increasing f_w, differences in the solvation environment increase, which can lead to conformational rearrangements and changes in the interplanar angle. The resulting decrease in the exciton conversion efficiency may be the reason for the shift of the S_0-S_2 bands from 488 to 501 nm. However, one should not exclude the possibility of the formation of a certain number of H-type aggregates with an absorption maximum at 501 nm.

There is no clear inflection point in the emission spectra of α,α-bis(BDP) recorded for THF-water mixtures, and with increasing water content, the fluorescence intensity gradually quenches to almost complete absence at f_w = 70 v/v % and higher (Figure 6c,d). When passing from pure THF to the THF-water mixture with f_w ≥ 80 v/v % and higher, the maximum of the emission band shifts from 648 nm to 662 nm. with a high probability, can be caused by a more polar solvation environment of α,α-bis(BDP) molecules. At f_w ≥ 80 v/v %, the maximum of the emission band shifts from 648 nm (in pure THF) to 662 nm, which can most likely be caused by the more polar solvation environment of α,α-bis(BDP) molecules.

Analysis of the decay curves (Figure 6f) showed that in mixtures with f_w = 70 v/v %, 93 v/v % and 95 v/v %, the fluorescence decay curves are described by three exponentials, compared to the monoexponential for the dye in pure THF. In addition to a small number of particles with a lifetime characteristic of a non-aggregated dye in pure THF (in the region of 3 ns and above), two more types of particles appear with significantly shorter lifetimes (approximately 0.5 ns and 0.25 ns), making the main contribution to the total time fluorescence lifetime (Table S4, *Supplementary Information*).

In order to estimate the dynamics of establishing equilibrium in the processes of aggregate formation, the absorption and fluorescence spectra of α,α-bis(BDP) in these mixtures were recorded every other day. In general, the nature of the spectral band is very similar to that obtained on the first day (Figure S5, *Supplementary Information*). There is a slight decrease in the absorption intensity of the

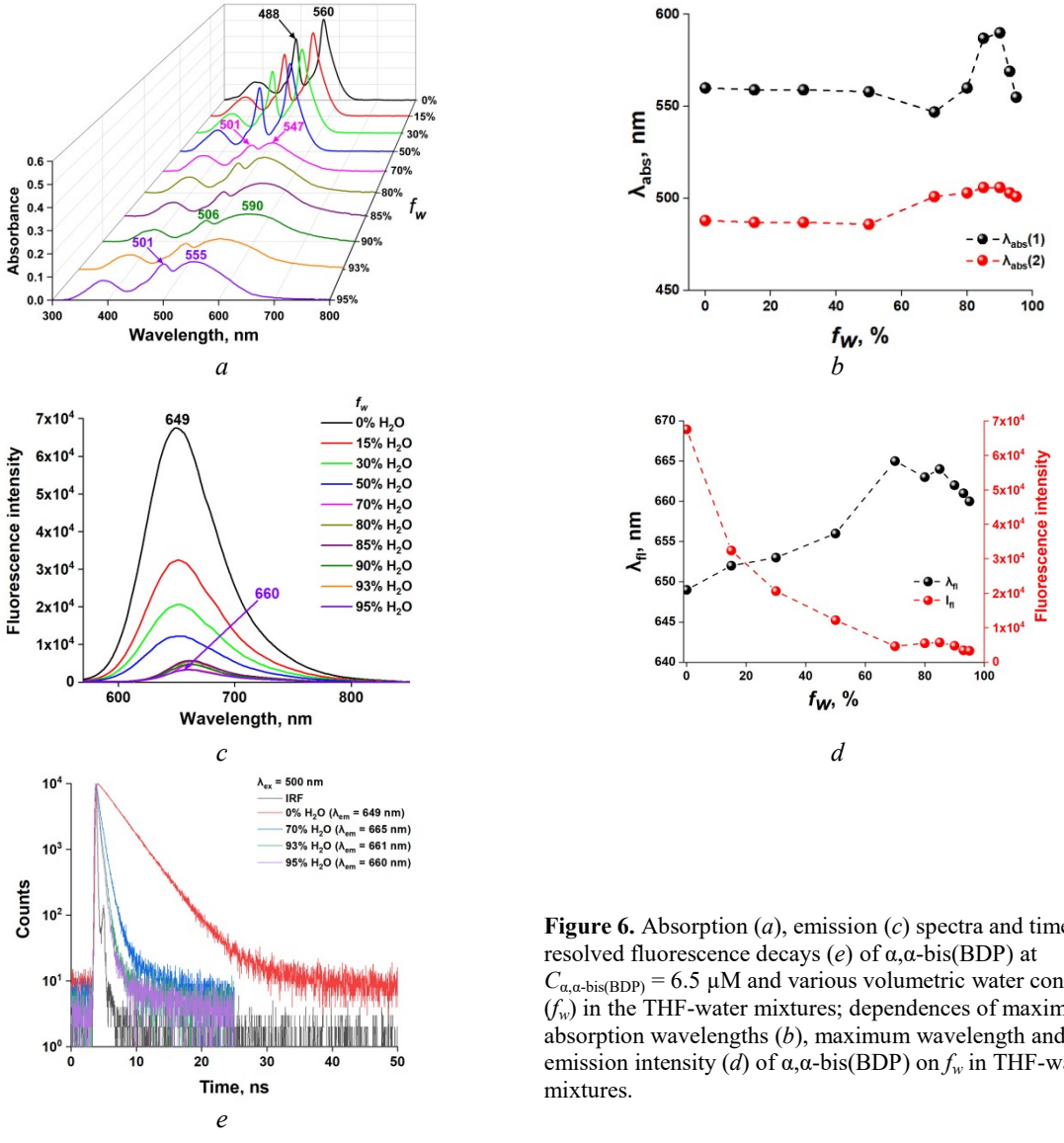

Figure 6. Absorption (*a*), emission (*c*) spectra and time resolved fluorescence decays (*e*) of α,α-bis(BDP) at $C_{α,α\text{-bis(BDP)}}$ = 6.5 μM and various volumetric water content (f_w) in the THF-water mixtures; dependences of maximum absorption wavelengths (*b*), maximum wavelength and emission intensity (*d*) of α,α-bis(BDP) on f_w in THF-water mixtures.

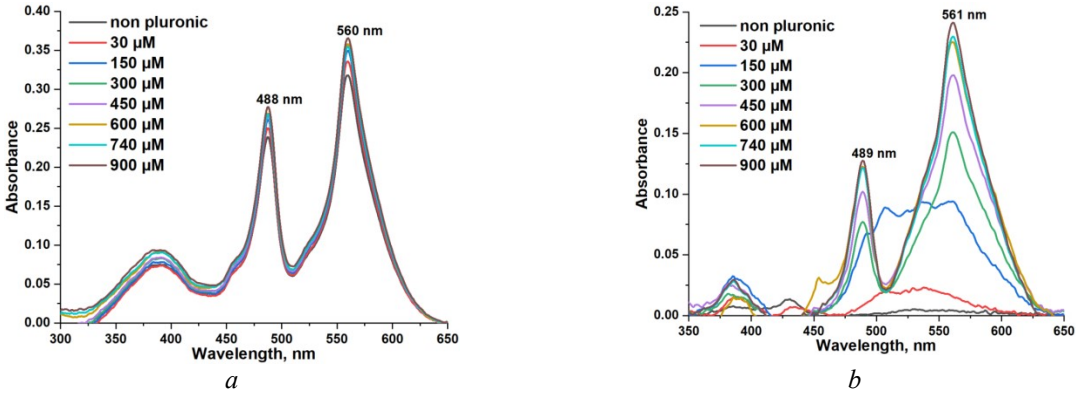

Figure 7. Absorption spectra of α,α-bis(BDP)@Pl in THF (a) and absorption spectra of α,α-bis(BDP)@Pl after dissolving the obtained films in PBS (p*H* 7.4), $C_{\alpha,\alpha\text{-bis(BDP)}}$ = 6.5 μM, the Pluronic® F127 content varied from 30 to 900 μM in the initial THF.

dye in mixtures with f_w > 50 v/v %, the maximum of the band in the blue region of the spectrum remains at 501 nm, and the maximum of the main band is located at 558 nm, which corresponds to the band of the non-aggregated dye in pure THF (559 nm) (Figure S5a). There is a noticeable additional fluorescence quenching in the fluorescence spectra.

The results of a study of the aggregation behavior of α,α-bis(BDP) in a THF-water mixture, as well as information about the high sensitivity of its photophysical characteristics to the nature of the solvation environment are demonstrated the need to develop the water-soluble forms of the dye for its delivery to cells when used as a photosensitizer.

α,α-Bis(BDP)@Pl water-soluble forms and their photophysical characterization

The most successful method for solubilizing BODIPYs has been found to be encapsulating the luminophore into micelles of amphiphilic block copolymers Pluronic®. It is known for its low toxicity and typically allows high solubilization efficiency while maintaining the important spectral properties of loaded photoactive compounds in an aqueous (physiological) environment. In earlier studies, was shown that even rather large molecules of bichromophores can be solubilized by micelles of the amphiphilic block copolymer Pluronic® F127.[12,17] Therefore, our first focus was to obtain water-soluble forms of α,α-bis(BDP) based on micelles of the amphiphilic block copolymer Pluronic® F127 as a biocompatible and popular solubilizer and passive drug delivery vehicle.[34] Solubilization was carried out by the "thin films" method, the advantage of which is to obtain time-stable solid forms of α,α-bis(BDP)@Pl that can be dissolved in buffer aqueous solutions and physiological media.

Series of solutions in THF were prepared with a constant dye concentration ($C_{\alpha,\alpha\text{-bis(BDP}}$ = 6.5 μM) and polymer content varying from deficiency to about 150-times excess (Figure 7a). An increase of polymer content leads to a slight increase of up to 10% in the absorption intensity of the dye. The films obtained after removing the solvent were dissolved in phosphate buffer p*H* 7.4 and spectra of the obtained solutions were analyzed as a dependence of the polymer content in the initial mixture. At polymer content of about 300 μM, the absorption spectrum (Figure 7b) conforming to α,α-bis(BDP) was recorded with S_0-S_1 and S_0-S_2 bands maxima at 489 nm and 561 nm, which is close to that of the original THF. On further increasing the polymer content up to 300 μM (close to the CMC value of Pluronic® F127), a significant increase in the intensity of the S_0-S_1 and S_0-S_2 maxima of the absorption bands of α,α-bis(BDP) was observed. Further increase of the content of Pluronic® F127 to 900 μM leads to an additional slight increase in the absorption intensity. The profile of the absorption spectrum of α,α-bis(BDP)@Pl in PBS is broadened compared to the initial spectra in THF perhaps due to partial association of the dye molecules.

The approximate solubilization efficiency of the dye calculated from the ratio of the limiting optical density at the maxima of the intense absorption band of α,α-bis(BDP)@Pl in the spectra in PBS and THF was 67%. The fluorescence lifetime of α,α-bis(BDP)@Pl recorded for the solution with C_{Pl} = 900 μM was 3.67 ns, which is comparable to that for nonpolar solvent solutions. The quantum yield of fluorescence was 29%.

The obtained results allow us to recommend the dye α,α-bis(BDP) for further researches for practical applications in various optical devices and biomedicine.

Conclusions

The halogen-free theranostic BODIPY–BODIPY dyad α,α-bis(BDP) with the functions of a photosensitizer and singlet oxygen generator was obtained. The α,α-bis(BDP) is characterized by high light absorption and effective excitonic interactions, near-red fluorescence and dual functionality due to relatively high fluorescence and singlet oxygen generation in aromatic and intermediate polarity solvents. The water-soluble form was obtained α,α-(bis(BDP)@Pl) by solubilization into Pluronic® F127 micelles. The results of the study in comparison with data for related α,α-CH_2-bis(BDP) dyads showed that, by varying the nature and the site of attachment BODIPY units, it is possible to finely tune the photo-physical characteristics of halogen-free bichromophoric photosensitizers for specific practical tasks. The resulting α,α-bis(BDP) and

α,α-bis(BDP)@Pl have gained importance in the biological field for their valuable spectroscopic properties.

Acknowledgements. This work was supported by Russian Science Foundation (grant No. 23-23-00206 *https://rscf.ru/project/23-23-00206/)*. The ^{1}H spectra and the time-resolved fluorescence measurements were carried out in the Centre of the scientific equipment collective use «The upper Volga region centre of physico-chemical research». MALDI mass spectra were obtained in the CSF-SAC FRC KSC RAS.

References

1. a) Bañuelos J. *Chem. Rec.* **2016**, *16*, 335; b) Bumagina N.A., Antina E.V., Ksenofontov A.A., Antina L.A., Kalyagin A.A., Berezin M.B. *Coord. Chem. Rev.* **2022**, *469*, 214684; c) Loudet A., Burgess K. *Chem.Rev.* **2007**, *107*, 4891.
2. Lu H., Mack J., Yang Y., Shen Z. *Chem. Soc. Rev.* **2014**, *43*, 4778.
3. Turksoy A., Yildiz D., Akkaya E.U. *Coord. Chem. Rev.* **2019**, *379*, 47.
4. Zhao J., Xu K., Yang W., Wang Z., Zhong F. *Chem. Soc. Rev.* **2015**, *44*, 8904.
5. Filatov M.A. *Org.Biomol. Chem.* **2019**, *18*, 10.
6. Gao M., Zeng Le, Jiang L., Zhang M., Chen Y., Huang L. *Molecules* **2023**, *28,* 5474.
7. a) Kandrashkin Y.E., Wang Z., Sukhanov A.A., Hou Y., Zhang X., Liu Y., Voronkova V.K., Zhao J. *J. Phys. Chem. Lett.* **2019**, *10*, 4157; b) Liu Y., Zhao J., Iagatti A., Bussotti L., Foggi P., Castellucci E., Di Donato M., Han K.-L. *J. Phys. Chem. C* **2018**, *122*, 2502; c) Zhang X.-F. *J. Photochem. Photobiol. A-Chem.* **2018**, *355*, 431.
8. Taguchi D., Nakamura T., Horiuchi H., Saikawa M., Nabeshima T. *J. Org. Chem.* **2018**, *83*, 5331.
9. a) Wu W., Zhao J., Sun J., Guo S. *J. Org. Chem.* **2012**, *77*, 5305; b) Zhang X.-F. *Dyes Pigm.* **2017**, *146*, 491; c) Cakmak Y., Kolemen S., Duman S., Dede Y., Dolen Y., Kilic B., Kostereli Z., Yildirim L.T., Dogan A.L., Guc D., Akkaya E.U. *Angew. Chem. Int. Ed.* **2011**, *50*, 11937.
10. Zhang X.-F., Yang X., Xu B. *PCCP* **2017**, *19*, 24792.
11. Ventura B., Marconi G., Bröring M., Krüger R., Flamigni L. *New J. Chem.* **2009**, *33*, 428.
12. Antina L.A., Kalinkina V.A., Sherudillo A.S., Kalyagin A.A., Lukanov M.M., Ksenofontov A.A., Berezin M.B., Antina E.V. *J. Lumin.* **2024**, *269*, 120411.
13. Bassan E., Gualandi A., Cozzi P.G., Ceroni P. *Chem. Sci.* **2021**, *12*, 6607.
14. Cao J., Zhang T., Sun W. *Dyes Pigm.* **2023**, *208*, 110797.
15. Kalyagin A., Antina L., Ksenofontov A., Antina E., Berezin M. *Int. J. Mol. Sci.* **2022**, *23*, 14402.
16. a) Guan Y., Shi J., Xia M., Zhang J., Pang Z., Marchetti A., Wang X., Cai J., Kong X. *Appl. Surf. Sci.* **2017**, *423*, 349; b) Gupta G., Sun Y., Das A., Stang P.J., Lee C.Y. *Coord. Chem. Rev.* **2022**, *452,* 214308; c) Lee Y.-R., Jang M.-S., Cho H.-Y., Kwon H.-J., Kim S., Ahn W.-S. *Chem. Eng. J.* **2015**, *271*, 276.
17. Antina L.A., Ravcheeva E.A., Dogadaeva S.A., Kalyagin A.A., Ksenofontov A.A., Bocharov P.S., Lodochnikova O.A., Islamov D.R., Berezin M.B., Antina E.V. *J. Photochem. Photobiol. A-Chem.* **2024**, *449*, 115370.
18. Antina L.A., Kalyagin A.A., Ksenofontov A.A., Pavelyev R.S., Lodochnikova O.A., Islamov D.R., Antina E.V., Berezin M.B. *J. Mol. Liq.* **2021**, *337*, 116416.
19. a) Kang Z., Wu Q., Guo X., Wang L., Ye Y., Yu C., Wang H., Hao E., Jiao L. *Chem. Commun.* **2021**, *57*, 9886; b) Stachelek P., Harriman A. *J. Phys. Chem. A* **2016**, *120*, 8104; c) Wang D., Wu Q., Zhang X., Wang W., Hao E., Jiao L. *Org. Lett.* **2020**, *22*, 7694.
20. a) Antina L.A., Bumagina N.A., Kalinkina V.A., Lukanov M.M., Ksenofontov A.A., Kazak A.V., Berezin M.B., Antina E.V. *Spectrochim. Acta A* **2022**, *278*, 121366; b) Dogadaeva S.A., Antina L.A., Ksenofontov A.A., Kalyagin A.A., Khodov I.A., Berezin M.B., Antina E.V., Pavelyev R.S., Frantsuzova L.V., Lodochnikova O.A., Islamov D.R. *J. Mol. Liq.* **2023**, *382*, 121892.
21. a) Hu W., Zhang R., Zhang X.-F., Liu J., Luo L. *Spectrochim. Acta A* **2022**, *272*, 120965; b) Wilkinson F., Helman W.P., Ross A.B. *J. Phys. Chem. Ref. Data* **1993**, *22*, 113; c) Spiller W., Kliesh H., Wohrle D., Hackbarth S., Roder B., Schnurpfeil G. *J. Porphyrins Phthalocyanines* **1998**, *2*, 145; d) Prieto-Castañeda A., García-Garrido F., Díaz-Norambuena C., Escriche-Navarro B., García-Fernández A., Bañuelos J., Rebollar E., García-Moreno I., Martínez-Máñez R., de La Moya S., Agarrabeitia A.R., Ortiz M.J. *Org. Lett.* **2022**, *24*, 3636; e) Pellosi D.S., Tessaro A.L., Moret F., Gaio E., Reddi E., Caetano W., Quaglia F., Hioka N. *J. Photochem. Photobiol. A-Chem.* **2016**, *314*, 143.
22. Bannwarth C., Ehlert S., Grimme S. *J. Chem. Theory Comput.* **2019**, *15*, 1652.
23. Chai J.-D., Head-Gordon M. *PCCP* **2008**, *10*, 6615.
24. Schäfer A., Horn H., Ahlrichs R. *J. Chem. Phys.* **1992**, *97*, 2571.
25. Marenich A.V., Cramer C.J., Truhlar D.G. *J. Phys. Chem. B* **2009**, *113*, 6378.
26. Frisch M.J., Trucks G.W., Schlegel H.B., Scuseria G.E., Robb M.A., Cheeseman J.R., Scalmani G., Barone V., Petersson G.A., Nakatsuji H., Li X., Caricato M., Marenich A.V., Bloino J., Janesko B.G., Gomperts R., Mennucci B., Hratchian H.P., Ortiz J.V., Izmaylov A.F., Sonnenberg J.L., Williams-Young D., Ding F., Lipparini F., Egidi F., Goings J., Peng B., Petrone A., Henderson T., Ranasinghe D., Zakrzewski V.G., Gao J., Rega N., Zheng G., Liang W., Hada M., Ehara M., Toyota K., Fukuda R., Hasegawa J., Ishida M., Nakajima T., Honda Y., Kitao O., Nakai H., Vreven T., Throssell K., Montgomery J.A., Peralta J.E., Ogliaro F., Bearpark M.J., Heyd J.J., Brothers E.N., Kudin K.N., Staroverov V.N., Keith T.A., Kobayashi R., Normand J., Raghavachari K., Rendell A.P., Burant J.C., Iyengar S.S., Tomasi J., Cossi M., Millam J.M., Klene M., Adamo C., Cammi R., Ochterski J.W., Martin R.L., Morokuma K., Farkas O., Foresman J.B., Fox D.J. *Gaussian 16, Revision B.01.* Gaussian, Inc., **2016**.
27. Nepomnyashchii A.B., Bröring M., Ahrens J., Bard A.J. *J. Am. Chem. Soc.* **2011**, *133*, 19498.
28. a) Bröring M., Krüger R., Link S., Kleeberg C., Köhler S., Xie X., Ventura B., Flamigni L. *Chem. Eur. J.* **2008**, *14*, 2976; b) Kasha M., Rawls H.R., Ashraf El-Bayoumi M. *Pure Appl. Chem.* **1965**, *11*, 371.
29. Giernoth R. *Angew. Chem. Int. Ed.* **2011**, *50*, 11289.
30. Nguyen V.-N., Yim Y., Kim S., Ryu B., Swamy K.M.K., Kim G., Kwon N., Kim C.-Y., Park S., Yoon J. *Angew. Chem. Int. Ed.* **2020**, *59*, 8957.
31. Liu Z., Jiang Z., Yan M., Wang X. *Front. Chem.* **2019**, *7*, 712.
32. a) Antina L.A., Ksenofontov A.A., Kazak A.V., Usol'tseva N.V., Antina E.V., Berezin M.B. *Colloids Surf., A* **2021**, *618*, 126449; b) Descalzo A.B., Ashokkumar P., Shen Z., Rurack K. *ChemPhotoChem* **2020**, *4*, 120.
33. Vu T.T., Dvorko M., Schmidt E.Y., Audibert J.-F., Retailleau P., Trofimov B.A., Pansu R.B., Clavier G., Méallet-Renault R. *J. Phys. Chem. C* **2013**, *117*, 5373.
34. a) Batrakova E.V., Kabanov A.V. *J. Controlled Release* **2008**, *130*, 98; b) de Castro K.C., Coco J.C., Dos Santos É.M., Ataide J.A., Martinez R.M., do Nascimento M.H.M., Prata J., da Fonte P.R.M.L., Severino P., Mazzola P.G., Baby A.R., Souto E.B., de Araujo D.R., Lopes A.M. *J. Controlled Release* **2023**, *353*, 802.

Received 12.04.2024
Accepted 23.04.2024